TWO- VERSUS THREE-DIMENSIONAL MELTING AND SPONTANEOUS REVERSING ISOMERIZATION IN ISOLATED SF_6–$(Ar)_9$ VAN DER WAALS CLUSTERS

John C. SHELLEY [1], Robert J. LE ROY
Guelph-Waterloo Centre for Graduate Work in Chemistry, University of Waterloo, Waterloo, Ontario, Canada N2L 3G1

and

François G. AMAR
Department of Chemistry, University of Maine, Orono, ME 04469, USA

Received 15 June 1988; in final form 16 August 1988

Molecular dynamics simulations for SF_6–$(Ar)_9$ clusters at effective temperatures in the range 5–45 K show that the system undergoes two different "melting" transitions, one at $T \approx 15$ K marking the onset of Ar atom mobility *within* a unimolecular layer around the SF_6, and a second at $T \approx 35$ K marking the onset of facile Ar atom motion out of and back into this layer. Moreover, on a narrow interval midway between these two points, the nine Ar atoms show a propensity for spontaneously isomerizing into and out of a long-lived *near-rigid* two-layer structure.

1. Introduction

The structural and dynamical propensities of van der Waals clusters are a subject of considerable fascination that has been attracting increasing attention in recent years. Questions such as what size such a cluster must have before it takes on the properties of the bulk material, what meaning conventional macroscopic concepts such as "phase" and "phase transition" have for clusters near or below this "macroproperty" size, and whether there exists more than one type of "melting" transition, are clearly of fundamental significance. The seminal work by Berry and co-workers on models of pure Ar clusters has helped us understand that in this context, the word "phase" refers to a class of cluster structures to which a given system belongs for a time interval much longer than either its characteristic vibrational periods or the time required for a transition from one form to the other [1–4]. Their work also delineated and explained the concept of "phase coexistence" for such systems. However, their "Lennard-Jonesium" model for $(Ar)_n$ is a very idealized system, and the cluster properties considered in those studies are not amenable to experimental observation. We have therefore undertaken studies of the mixed van der Waals clusters SF_6–$(Ar)_n$, systems for which excellent models for both the intermolecular interactions [5–7] and the "cluster shift" of the infrared monomer spectra [7] have been developed, and for which experimental data are available [8–10].

In our previous work on this topic, a model for predicting the perturbation of vibration–rotation levels of SF_6 by neighbouring Ar atoms was developed and tested [7]. Monte Carlo methods were then used to average those shifts over a canonical ensemble of cluster structures to predict the thermally averaged perturbed infrared spectrum of an SF_6 molecule solvated with from 1 to 100 Ar atoms at 30 or 50 K. A bimodal splitting of the spectral peaks for certain cluster sizes was initially associated with phase coexistence [11], but later recognized as being due to the symmetry of the cluster structure when a

[1] Present address: Department of Chemistry, University of Pennsylvania, Philadelphia, PA 19104, USA.

0 009-2614/88/$ 03.50

nearly complete layer of Ar atoms is wrapped around the SF_6 chromophore [12]. At the same time, other aspects of those simulations pointed to the existence (and possibly co-existence) of two different classes of cluster structures which had distinctly different properties [7]. However, in the absence of dynamical studies, no firm conclusions could be reached.

The present paper is a preliminary report of the results of molecular dynamics studies of SF_6–$(Ar)_n$ clusters for a wide range of energies [13]. In the following, section 2 describes the methodology on which the present study is based; section 3 summarizes aspects of our results for the "$n=9$" clusters SF_6–$(Ar)_9$, and section 4 presents our conclusions.

2. Methodology

As in our previous studies [7,11,12], the potential energy of the SF_6–$(Ar)_9$ system was represented as a pairwise sum based on an inverse-power-sum approximation to the Ar–Ar potential of Aziz and Slaman [6], plus the full anisotropic SF_6–Ar potential of Pack et al. [5]. The molecular dynamics program was adapted from one originally devised for simulating photodissociation in clusters [14]. The equations of motion were integrated using a fourth-order Adams–Moulton predictor–corrector method initialized with four iterations of Runge–Kutta integration [15,16]. The time step used in the numerical integration was 0.0025 ps; this value sufficed to ensure that in our 1.5 ns runs, the total energy was typically conserved to 1 part in 10^5, with the worst deviation encountered being less than 2 parts in 10^3.

The first molecular dynamics run for an SF_6–$(Ar)_n$ cluster of a given size was started from an equilibrated configuration yielded by a 30 K Monte Carlo calculation [7]. A set of momenta was generated using the Box–Muller method [17], a procedure which yields a random distribution of values consistent with the desired temperature (or average kinetic energy). The centre-of-mass position and velocity were then calculated and subtracted from the values for the individual particles. Similarly, any initial net angular momentum of the cluster was removed before the start of each run. This latter step was necessary because properties such as the "mean-square displacement" (see below) are more difficult to calculate in a meaningful way for rotating clusters.

Subsequent runs for a given cluster size were sometimes started independently in the manner described above, but more often were started by initializing the particle positions and momenta at the values attained at the end of a molecular dynamics run for a neighbouring value of the toal energy, and then scaling the momenta to achieve the desired total energy. This scaling step does not change the total angular momentum if it was initially zero. In a typical simulation, a relaxation interval of 100–200 ps (or 40000–80000 time steps) separated the initiation of the run from the start of the data collection.

Although the clusters considered here are isolated or microcanonical species, energy equipartition arguments allow one to associate an effective cluster temperature with the average value of the total system kinetic energy $\langle E_{\mathrm{kin}} \rangle$:

$$T = \langle E_{\mathrm{kin}} \rangle / \tfrac{3}{2} n k_{\mathrm{B}}, \qquad (1)$$

where k_{B} is Boltzmann's constant and n is the number of Ar atoms in the cluster. A variety of other structural and dynamical properties were also calculated during the course of each run, including radial distribution functions, the kinetic energy distribution, root-mean-square bond length fluctuations, and features of the infrared spectrum, as well as more explicitly time-dependent properties such as the mean-square particle displacement as a function of time [1].

As in our earlier work, the spectroscopic property being monitored is the frequency of the triply degenerate fundamental of the ν_3 band of the solvated SF_6 chromophore. Using a simple yet accurate method for predicting the shift of this band occurring when the SF_6 molecule is perturbed by neighbouring atoms [7], it has been shown that this spectrum is quite sensitive to the manner in which the Ar atoms are packed about the SF_6 chromophore [7,12,13]. It is therefore a very appropriate tool for probing the properties and behaviour of these clusters.

3. Molecular dynamics simulations of SF_6–$(Ar)_9$ clusters

3.1. Two- versus three-dimensional melting

Molecular dynamics runs of (typically) 1500 ps were performed for SF_6–$(Ar)_9$ clusters at total energies E_{tot} corresponding to effective temperatures (see eq. (1)) ranging from 5 to 45 K. Fig. 1 shows that the "caloric curve", a plot of $\langle E_{kin} \rangle$ versus E_{tot}, is a well-behaved monotonic function consisting of two near-linear segments meeting at an effective temperature near 30 K. Since the slope of the caloric curve defines the heat capacity of the system, conventional macroscopic system reasoning would suggest that a phase transition occurs at that point. However, examination of microscopic dynamical properties of the system (see below) shows that this is *not* the case.

Although E_{tot} is the actual independent variable characterizing a given run, the effective temperature determined from the average kinetic energy is clearly a more intuitively meaningful parameter. This temperature, as defined by eq. (1) (see also fig. 1), is therefore used as the independent variable in most of the following.

Fig. 2A presents a plot of the relative root-mean-square bond length fluctuation, averaged over all of

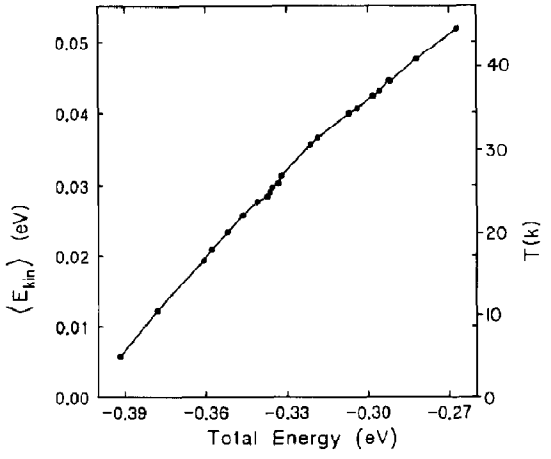

Fig. 1. Caloric curve for SF_6–$(Ar)_9$ clusters, as generated from 1.5 ns molecular dynamics runs at the indicated total energies; the temperature scale on the axis at the right-hand side was generated using eq. (1).

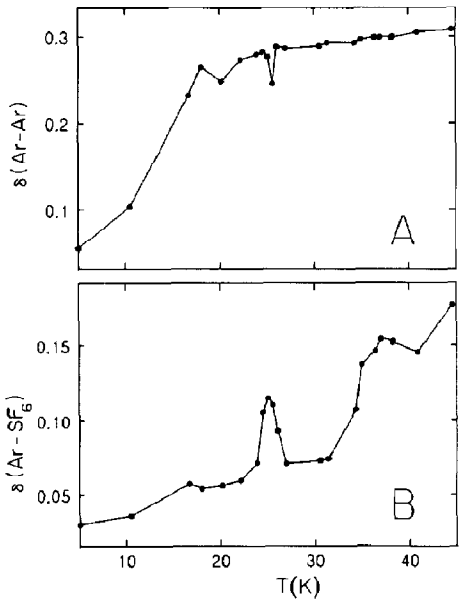

Fig. 2. Averaged relative root-mean-square bond length fluctuations for the Ar–Ar (A) and Ar–SF_6 (B) distances in an SF_6–$(Ar)_9$ cluster, calculated in 1.5 ns molecular dynamics runs.

the Ar–Ar pair separations in the cluster:

$$\delta(\mathrm{Ar\text{–}Ar}) = \frac{2}{n(n-1)} \sum_{i<j=1}^{n} \frac{[\langle R_{ij}^2 \rangle_t - \langle R_{ij} \rangle_t^2]^{1/2}}{\langle R_{ij} \rangle_t}, \tag{2}$$

where $\langle \ \rangle_t$ implies a time average along the entire trajectory, $R_{ij} = |\boldsymbol{R}_i - \boldsymbol{R}_j|$ is the distance between atoms i and j, and n $(=9)$ is the number of Ar atoms in the cluster. The Lindemann criterion for melting suggests that a solid→liquid transition occurs when this quantity passes through a value of approximately 0.1 [18]. Beck et al. [3] argue that for clusters, this criterion may lead to estimates of the melting temperature which are slightly low. However, from the rapid rise seen in fig. 2A, it seems clear that the nine Ar atoms in our clusters are definitely displaying the kind of wide amplitude motion associated with a liquid at temperatures $T \gtrsim 15$ K.

Further evidence regarding the occurrence of a "melting" transition at around 15 K is provided by plots of the mean-square particle displacement as a function of time [1]:

$$\langle R^2 \rangle_t = \frac{1}{n} \sum_{j=1}^{n} |\boldsymbol{R}_j(t+t_0) - \boldsymbol{R}_j(t_0)|^2. \tag{3}$$

For macroscopic systems, the "long-time" (i.e. $5 \lesssim t \lesssim 15$ ps) slope of a plot of this type defines a diffusion coefficient for the system. For the present case, distinct positive slopes are obtained for runs corresponding to $T \geqslant 17$ K, but were not evident for a run at 11 K. This observation confirms the conclusion implied by fig. 2A that melting has occurred by $T \approx 15$ K [13].

In contrast with the above, the plot of the root-mean-square fluctuations of the Ar–SF_6 bond lengths, seen in fig. 2B, suggests that as far as the motion of the Ar's relative to the SF_6 is concerned, melting *does not occur until* $T \gtrsim 35$ K. Further evidence regarding this point is provided by the behaviour of the average Ar–SF_6 bond lengths, plotted in fig. 3A. Ignoring (for the moment) the narrow spike at 25.6 K, this plot shows that the average Ar–SF_6 distance increases very gradually with temperature for the colder clusters, but undergoes an abrupt change to a much more rapid growth rate by $T = 34$ K.

Since the Ar–SF_6 pair potential is considerably stronger than that for Ar–Ar [5,6], it is reasonable to expect that at low temperatures the Ar atoms would lie in a single layer on the surface of the SF_6, while multilayered structures would become increasingly accessible to the warmer clusters. The above results make it clear that this three-dimensional melting does not occur until $T \gtrsim 35$ K, although the two-dimensional melting which allows the Ar atoms to move around *within* an incomplete close-packed layer wrapped around the SF_6 occurs at $T \approx 15$ K.

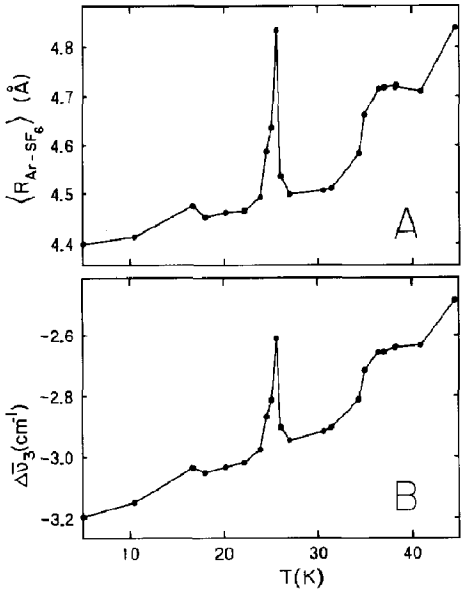

Fig. 3. (A) Average of the Ar–SF_6 distances, calculated for 1.5 ns molecular dynamics runs. (B) Average frequency shift of the fundamental ν_3 band of SF_6, averaged over a 1.5 ns molecular dynamics run.

3.2. Spontaneous reversing isomerization of an isolated cluster

The peak near 26 K seen in figs. 2B and 3A, together with the slight irregularity of the caloric curve of fig. 1 in this same region, suggests that some new type of behaviour is occurring there. Further evidence of this is provided by the behaviour of the predicted average ν_3 frequency shift, $\overline{\Delta\nu_3}(T)$, plotted in fig. 3B. According to the model of ref. [7], the contribution of a given Ar atom to this average frequency shift is proportional to $1/(R_{\mathrm{Ar-SF_6}})^6$, and is approximately additive for the several Ar atoms in a cluster. Thus, the similarity of the plots in the two segments of fig. 3 should not be surprising. However, in view of the success of this model [7], this does confirm that the infrared spectrum should indeed be a sensitive probe of the structure of these small clusters.

The sharp peaks in the plots seen in fig. 3 indicate that at temperatures near 26 K, one or more of the Ar atoms spend a substantial amount of time farther from the SF_6 than the others do. This observation is confirmed by the form of the Ar–SF_6 radial distribution functions for these simulation runs. Those for temperatures very near 25.6 K show a distinct second peak at around 7 Å while those for lower and (neighbouring) higher temperatures show only the main peak at 4.5 Å. Due to the modest length (1.5 ns) of these runs, some features of this behaviour may be artifacts of incomplete statistical sampling, and may not represent equilibrium behaviour. However, it is still clear that this structure signals the presence of unusual cluster behaviour.

One question raised by the above result is whether a cluster at 25.6 K retains a multilayer structure throughout the run, and if not, whether the residence times in its alternative forms are long compared to the periods for other characteristic motions of the system. This point is addressed by the upper seg-

ment of fig. 4, which shows how locally averaged frequency shifts (calculated at 0.5 ps intervals and then averaged in groups of five) evolve as the simulation progresses. The equilibrium structure of these clusters consists of an incomplete close-packed unimolecular layer of Ar atoms wrapped around the SF_6 [12,13]; this is the form characterized by the frequency shift of $-3\ cm^{-1}$ seen at the beginning of this plot. Since the magnitude of the frequency shift is approximately proportional to the number of Ar atoms in contact with the SF_6 [7], this figure suggests that the system spends an initial 410 ps period in a one-layer type of structure, and then isomerizes to a two-layer form in which one third of the Ar atoms are displaced relatively far from the SF_6 and the associated frequency shift is only slightly greater than $-2\ cm^{-1}$. Following a sojourn of ≈ 700 ps in this second form, the displaced Ar atoms then return to the original one-layer form.

The nature of the cluster structures associated with

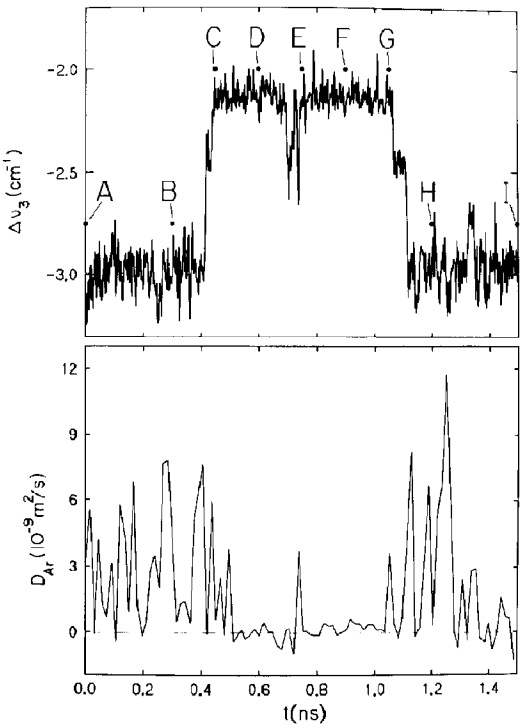

Fig. 4. Upper segment: for a molecular dynamics run at $E_{tot} = -0.33544$ eV (or $T = 25.6$ K), evolution of the averaged ν_3 frequency shift with time. Lower segment: for the same run, locally averaged values of the Ar atom diffusion coefficient in the cluster.

the two characteristic frequency shift regions is illustrated by fig. 5, which shows the structures corresponding to the labelled points on the upper segment of fig. 4. While the views were chosen for illustrative clarity, the axes drawn in the lower right-hand corner of each figure segment represent a right-handed coordinate system fixed on the SF_6 molecule. These results show that at 25.6 K ($E_{tot} = -0.33544$ eV) the isolated cluster can undergo spontaneous isomerization from one-layer structures in which the Ar atoms form a close-packed unimolecular layer wrapped around the SF_6, *into and* (following a significant residence time) *back out of* a two-layer structure in which the Ar atoms are piled up on one end of the molecule.

The dynamical properties of these two classes of structures are also quite different. This is evidenced by the permutations (or lack thereof) of the Ar atoms seen in the structures of fig. 5. They show that in the one-layer regions associated with the 3 cm^{-1} frequency shift, the Ar atoms are undergoing the kind of continuous rearrangement expected of a liquid. In contrast, in the two-layer region their *relative arrangement remains fixed*, although this Ar atom "cap" is clearly (see structures) undergoing wide amplitude vibrational motion. Thus, this isomerization appears to involve a change from a class of two-dimensional liquid-like $(Ar)_9$ structures, to a solid-like cap of Ar's undergoing wide amplitude vibrational motion. In both cases, the Ar-atom cap undergoes continuous rotation relative to the (distinctly non-spherical [5,7]) SF_6 molecule. This latter point is illustrated by the evolution of the axes in segments C–G of fig. 5.

Further evidence regarding the solid-like nature of the two-layer structures is provided by a value for the root-mean-square Ar–Ar bond length fluctuation calculated for the portion of the simulation run associated with the two-layer structures. The value of δ(Ar–Ar) obtained in this way was 0.073, well below the value of 0.1 which the Lindemann criterion associates with melting transitions [18].

The behaviour of Ar atom diffusion coefficients calculated from the long-time behaviour of the mean-square particle displacement of eq. (3) [1,12,13] also confirms this conclusion. Following the procedure of ref. [1], mean-square Ar atom displacement curves were collected and averaged for several con-

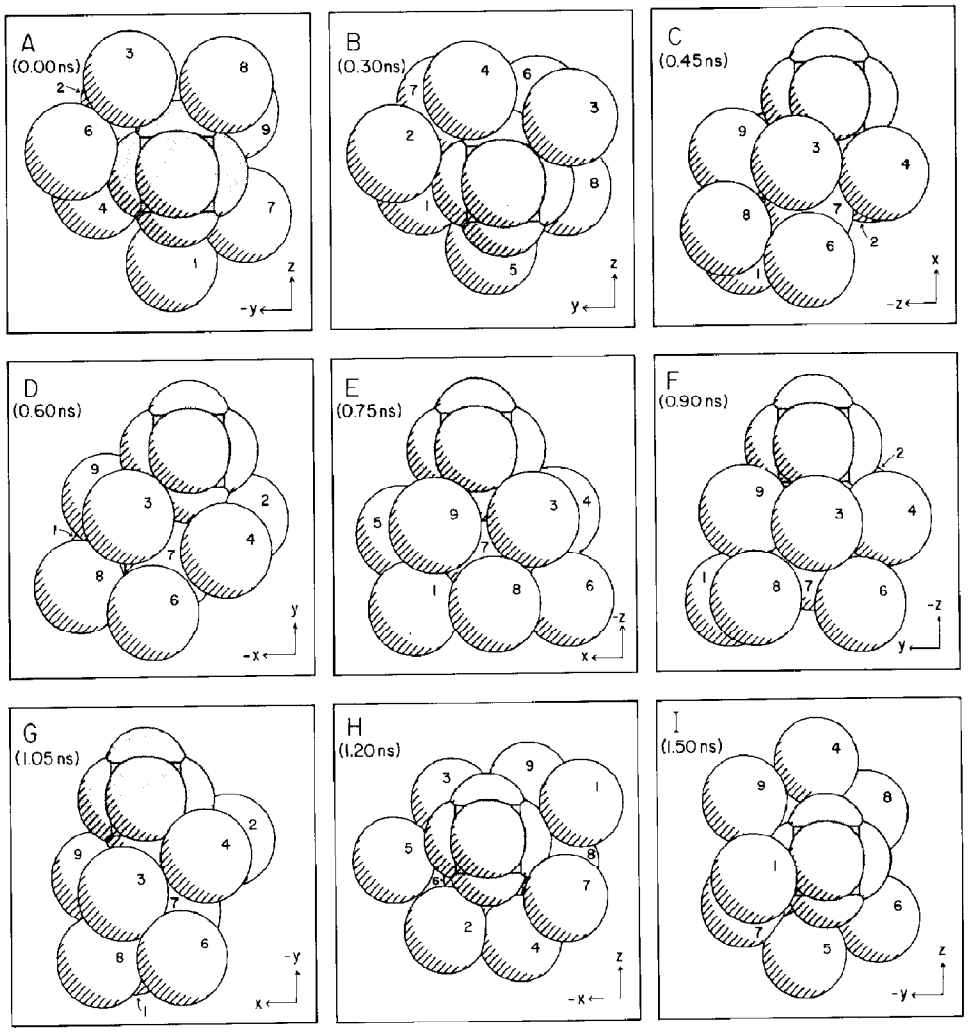

Fig. 5. SF_6–$(Ar)_9$ cluster structures for the 25.6 K molecular dynamics run, taken at times corresponding to the labeled points in the upper segment of fig. 4. The SF_6 molecule is shaded and the Ar atoms numbered. The axes shown represent a coordinate system fixed on the SF_6 molecule.

secutive 15 ps intervals, and the resulting long-time slope used to define a diffusion coefficient point in the lower segment of fig. 4. The noise in this plot reflects both the inherent statistical noise of these calculations and the ambiguity associated with the notion of a diffusion coefficient in a finite system. However, it is still clear that in the time interval associated with the smaller (2 cm^{-1}) frequency shift, the diffusion rate is more than an order of magnitude slower than at other times. Thus, it seems clear that across this middle interval, the Ar atom cap is behaving like a solid, in that *no rearrangements occur* for a time interval much longer than either the characteristic (ps) vibrational periods of the cluster or the time required for the transitions from or to the one-layer liquid-like form.

Two further questions which arise regarding the two-layer structure concern its absolute energy relative to that of the one-layer "equilibrium" structure, and the height of the barrier separating it from the latter. Applying the same annealing techniques used for determining the equilibrium structures [13], the energy minimum for the fully quenched two-layer structure was found to be −0.40251 eV, a value only

11.0 cm^{-1} higher than the absolute energy minimum found for the close-packed one-layer structures. An upper limit to the height of the potential barrier separating these two minima was then empirically defined as the lowest total energy for which a molecular dynamics run originating in the quenched two-layer configuration *failed to escape* to the (dominant) one-layer form during a 2 ns molecular dynamics run. This energy was found to be -0.354 eV, a value which implies that the saddle point separating these two structures lies less than 390 cm^{-1} above this second minimum. Because it is statistically *im*probable that our first observed "escape trajectory" at $E_{tot} = -0.353$ eV followed the minimum energy path, the actual barrier may be considerably lower than this. However, this same consideration, together with the fact that a considerably larger volume of phase space appears to be available to the one-layer structures, explains why the two-layer structures did not manifest themselves in our original 1.5 ns runs at energies below $E_{tot} = -0.340$ eV ($T = 24$ K).

4. Discussion and conclusions

While the results described above are very intriguing, they are of course preliminary. In particular, the significance of the sharp drop-off on the high-energy side of the peak at 25.6 K in figs. 2B and 3 is not entirely clear. To address this question, long runs will have to be performed at a range of energies to determine whether the kind of long-lived isomerization observed here recurs either regularly or frequently, and whether its occurrence is indeed confined to a very narrow range of energies. As a first step in this direction, the run at $E_{tot} = -0.33544$ eV ($T = 25.6$ K) which was the source of the results shown in figs. 4 and 5 was continued for another 12 ns, and an additional run starting from an independent set of particle momenta made at the same total energy. The analogs of the upper segment of fig. 4 for those cases showed a number of one- and two-Ar-atom excursions into a second layer which lasted for a significant fraction of a nanosecond, but they showed no recurrence of the very long-lived three-atom double layer seen in segments C–G of fig. 5. However, the analogous frequency shift plot for one of the neighbouring energies *did* show an excursion into this type of three-atom two-layer structure which lasted for more than 130 ps. Thus, it appears that while this particular type of excursion does not recur frequently, it is not an isolated occurrence.

The non-recurrence of the three-atom two-layer structures in the extended runs mentioned above shows that we have not obtained proper statistical averages of the possible behaviour of the system at effective temperatures near 25.6 K. This point is confirmed by the fact that the two-layer structures were not observed in our initial 1.5 ps runs for energies below -0.337 eV, although they fall apart on a nanosecond time scale for energies above -0.353 eV. This implies that the two-layer structures are only accessed from the one-layer structures via a narrow bottleneck in phase space. One possible explanation of the drop-off on the high-temperature side of the peaks in figs. 2B and 3 would then simply be that by accident, the trajectories at energies near -0.337 eV found this bottleneck while those at slightly higher (and lower) energies did not. An alternate interpretation, however, is that the width of the bottleneck in phase space increases very rapidly with energy, causing the two-layer structures to become very short-lived when the energy is increased further. In this case, although higher energy trajectories would readily access these two-layer structures, residence time there would be very short, and since they occupy only a small fraction of the phase space available at this energy, the averaged properties would largely reflect the dominant one-layer form.

In any case, it is clear that further studies to better delineate the nature of this isomerization behaviour and ascertain its dependence on the details of the relevant intermolecular potentials would be most fruitful. In this regard, the steepest descent quenching technique of Amar and Berry [2] should prove useful for determining the relative importance of the different types of isomers as a function of energy, while the procedure of Berry, Davis and Beck [19] should prove useful for characterizing the barrier(s) separating them. Certainly, the longevity and very different spectroscopic properties of the two classes of structures makes their observation a very tantalizing possibility.

The existence of different melting temperatures for different types of solvent motion in mixed clusters has been independently inferred by Leutwyler and

Bösiger from Monte Carlo studies of carbazole–$(Ar)_n$ clusters [20,21]. However, since the cluster energy varies along the Markov chain associated with the Monte Carlo simulation, it is not clear how well this should mimic the behaviour of the isolated clusters seen experimentally [20,21]. In any case, the contrast between the Ar–Ar and Ar–SF_6 bond length fluctuation curves seen in the present fig. 2 clearly delineates the existence of separate melting temperatures for two- and three-dimensional motion of the Ar atoms in the SF_6–$(Ar)_n$ system.

The results shown in figs. 4 and 5, demonstrating the ability of our isolated cluster to move between very different long-lived types of structures, are reminiscent of the sort of "phase coexistence" behaviour delineated by Berry and co-workers for pure Ar clusters [1–4]. However, there are significant differences. In particular, in the work on the pure Ar clusters, the coexistence is between vibrationally hot ground-state equilibrium structures and the more irregular class of structures accessed when Ar atoms first become mobile. In contrast, in the present case, the solid-like structures in question are *not* vibrationally distorted ground-state equilibrium structures, and are not simply related to them; they have very different configurations. Moreover, access to them from the one-layer liquid-like structures generated by the first melting transition only becomes possible as the total energy (and the effective temperature) *increases*. In other words, in the present case one must "heat" the liquid-like one-layer clusters to obtain access to the solid-like two-layer structures! If the type of "first-melting" phase coexistence behaviour studied by Berry and co-workers [1–4] does occur in the present system, it should be found on the interval from 11 to 17 K; while its existence is by no means ruled out, it would represent a different type of phenomenon than that reported here.

In conclusion, therefore, the picture which is emerging for our SF_6–$(Ar)_9$ clusters appears to be as follows. The minimum energy structure consists of a close-packed unimolecular layer of Ar atoms wrapped (incompletely) around the SF_6. It has very soft modes of vibration which on warming open up to allow facile Ar atom rearrangements (or melting) *within* this layer at temperatures around 15 K. There also exists a class of two-layer structures with almost the same potential energy minimum as the ground state. However, they appear to have much higher characteristic frequencies and an ensuing relatively low density of states, a fact demonstrated by the very different δ(Ar–Ar) values of 0.28 and 0.073, respectively, associated with the one- and two-layer portions of the simulation considered in figs. 4 and 5. While transitions between these classes of structures are possible for total energies of -0.353 eV (and probably considerably below that), statistical considerations made it difficult to observe them on a nanosecond time scale until the total energy reaches around -0.34 eV. Thus, there appears to be a significant bottleneck in phase space hindering interconversion of these two types of structures. Finally, at total energies corresponding to temperatures of around 35 K, a broad range of multilayer structures eventually become readily accessible and full three-dimensional melting occurs. Heating the system further then leads to fragmentation on a nanosecond time scale at temperatures around 45 K.

Acknowledgement

We are grateful to Ms. Lejla Babic for assistance with some of the calculations. This research was supported by the Natural Sciences and Engineering Research Council of Canada.

References

[1] J. Jellinek, T.L. Beck and R.S. Berry, J. Chem. Phys. 84 (1986) 2783.
[2] F.G. Amar and R.S. Berry, J. Chem. Phys. 85 (1986) 5943.
[3] T.L. Beck, J. Jellinek and R.S. Berry, J. Chem. Phys. 87 (1987) 545.
[4] R.S. Berry, in: Large finite systems, Proceedings of the 20th Jerusalem Symposium on Quantum Chemistry and Biochemistry, eds. J. Jortner and B. Pullman (Reidel, Dordrecht, 1987) pp. 135–143.
[5] R. T Pack, J.J. Valentini and J.B. Cross, J. Chem. Phys. 77 (1982) 5486.
[6] R.A. Aziz and M.J. Slaman, Mol. Phys. 58 (1986) 679.
[7] D. Eichenauer and R.J. Le Roy, J. Chem. Phys. 88 (1988) 2898.
[8] T.E. Gough, D.G. Knight and G. Scoles, Chem. Phys. Letters 97 (1983) 155.
[9] T.E. Gough, M. Mengel, P.A. Rowntree and G. Scoles, J. Chem. Phys. 83 (1985) 4958.

[10] X. Gu, B. Zhang, N. Isenor and G. Scoles, private communication (1987).
[11] D. Eichenauer and R.J. Le Roy, Phys. Rev. Letters 57 (1986) 2920.
[12] R.J. Le Roy, J.C. Shelley and D. Eichenauer, in: Large finite systems, Proceedings of the 20th Jerusalem Symposium on Quantum Chemistry and Biochemistry, eds. J. Jortner and B. Pullman (Reidel, Dordrecht, 1987) pp. 165–172.
[13] J.C. Shelley, M.Sc. Thesis, University of Waterloo (1987), University of Waterloo Chem. Phys. Res. Rept. CP-322 (1987).
[14] F.G. Amar and B.J. Berne, J. Phys. Chem. 88 (1984) 6720.
[15] C.F. Gerald, Applied numerical analysis (Addison-Wesley, Reading, 1984) ch. 6, par. 6.
[16] J. Kashick and B.J. Berne, in: Modern theoretical chemistry, Vol. 6. Statistical mechanics, part B. Time-dependent processes, ed. B.J. Berne (Plenum Press, New York, 1977) p. 41.
[17] W.H. Press, B.P. Flannery, S.A. Teukolsky and W.T. Vetterling, Numerical recipies – the art of scientific computing (Cambridge Univ. Press, Cambridge, 1986) sect. 7.2.
[18] I.I. Frenkel, Kinetic theory of liquids (Dover, New York, 1955).
[19] R.S. Berry, H.L. Davis and T.L. Beck, Chem. Phys. Letters 147 (1988) 13.
[20] S. Leutwyler and J. Bösiger, in: Large finite systems, Proceedings of the 20th Jerusalem Symposium on Quantum Chemistry and Biochemistry, eds. J. Jortner and B. Pullman (Reidel, Dordrecht, 1987) pp. 153–164.
[21] J. Bösiger and S. Leutwyler, Phys. Rev. Letters 59 (1987) 1895.